minerals

MDPI

Article

Clean Utilization of Limonite Ore by Suspension Magnetization Roasting Technology

Jianping Jin [1,2], Xinran Zhu [1,2], Pengchao Li [1,2,*], Yanjun Li [1,2] and Yuexin Han [1,2]

[1] School of Resources and Civil Engineering, Northeastern University, Shenyang 110819, China; jinjianping@mail.neu.edu.cn (J.J.); zhuxinran@mail.neu.edu.cn (X.Z.); liyanjun@mail.neu.edu.cn (Y.L.); dongdafulong@mail.neu.edu.cn (Y.H.)

[2] National-Local Joint Engineering Research Center of High-Efficient Exploitation Technology for Refratory Iron Ore Resources, Shenyang 110819, China

* Correspondence: 1910369@stu.neu.edu.cn

Abstract: As a typical refractory iron ore, the utilization of limonite ore with conventional mineral processing methods has great limitations. In this study, suspension magnetization roasting technology was developed and utilized to recover limonite ore. The influences of roasting temperature, roasting time, and reducing gas concentration on the magnetization roasting process were investigated. The optimal roasting conditions were determined to be a roasting temperature of 480 °C, a roasting time of 12.5 min, and a reducing gas concentration of 20%. Under optimal conditions, an iron concentrate grade of 60.12% and iron recovery of 91.96% was obtained. The phase transformation, magnetism variation, and microstructure evolution behavior were systematically analyzed by X-ray diffraction, vibrating sample magnetometer, and scanning electron microscope. The results indicated that hematite and goethite were eventually transformed into magnetite during the magnetization roasting process. Moreover, the magnetism of roasted products significantly improved due to the formation of ferrimagnetic magnetite in magnetization roasting. This study has implications for the utilization of limonite ore using suspension magnetization roasting technology.

Keywords: clean utilization; suspension magnetization roasting; limonite ore; phase transformation; magnetism

Citation: Jin, J.; Zhu, X.; Li, P.; Li, Y.; Han, Y. Clean Utilization of Limonite Ore by Suspension Magnetization Roasting Technology. *Minerals* **2022**, *12*, 260. https://doi.org/10.3390/min12020260

Academic Editors: Chiharu Tokoro, Shigeshi Fuchida and Yutaro Takaya

Received: 13 January 2022
Accepted: 14 February 2022
Published: 17 February 2022

1. Introduction

As an abundant element on Earth, iron plays a vital role in industrial production and ranks first in the world's metal consumption [1–3]. In the development process of the steel industry, iron ore is an indispensable and crucial industrial raw material [4,5]. Relevant statistics show that there are currently more than 800 billion tons of iron ore globally, including 230 billion tons of iron. However, the annual consumption of iron ore in the steel industry has increased up to 2.6 billion tons [6]. Considering the rapid depletion of high-grade iron ore resources, the enrichment of low-grade iron ore in the form of limonite, siderite, pyrite, etc., with poor endowment and no compliance with smelting requirements has been further investigated [7–11].

Diverse mineral components, complex associated relationships between minerals, and low-grade useful components are the main characteristics of refractory low-grade iron ore. Moreover, the common impurity elements silicon, aluminum, and phosphorus in the refractory iron ore mostly exist in the form of alumina, kaolinite, aluminosilicate, chlorite, iron silicate, and iron olivine, and are complexed with iron minerals [12–14]. Currently, solvable methods for the efficient beneficiation of refractory low-grade iron ore are further discussed, such as improving mineral liberation and developing highly efficient separation processes, which have been explored to enhance refractory low-grade iron ore separation [15–17]. In addition, some scholars have paid great attention to optimizing traditional beneficiation techniques to improve the grade of refractory low-grade iron

ore. Froth flotation is an effective method to recover fine iron minerals, and numerous investigations have been carried out on the recovery of refractory low-grade iron ore, especially for fine-grained iron minerals [18–23]. Some specific flotation schemes, such as shear flocculation flotation and carrier flotation, have been used to recover refractory low-grade ore [24,25]. However, the limitations of separation efficiency and product quality are the main problems in flotation. The technologies mentioned above promote the enrichment of refractory low-grade iron ore. However, due to the complexity of the nature of low-grade iron ore, these methods are limited to laboratory studies and far from satisfactorily meeting the requirements of industrialized scale production.

As a common and widely distributed iron oxide ore resource, limonite ore is a typical refractory low-grade iron ore. In addition to the common characteristics of refractory low-grade iron ore, high crystal water content, loose structure, and easy sliming are the distinctive properties of limonite ore. Due to complex mineralogy, it is difficult to beneficiate limonite ore by traditional technologies such as gravity separation, magnetic separation, and flotation [26–29]. Furthermore, approximately 1.2 billion tons of limonite resources in China have not been effectively exploited. Compared with conventional mineral processing technologies, magnetic roasting with a low-intensity magnetic separation process is an effective method for recovering refractory low-grade iron ore. According to the different reduction substances in the magnetization roasting process, the existing magnetization roasting technologies include carbothermal reduction roasting, sulfur-based roasting reduction, inorganic roasting reduction, and organic roasting reduction. Among them, carbothermal reduction roasting technology has been extensively studied, and it is a mature magnetized roasting process [30–34]. However, the existing carbothermal reduction roasting process has higher requirements for the quality of the reducing agent and has the disadvantages of high energy consumption and being a greater threat to the environment [35]. Recently, suspension magnetization roasting technology, which has the characteristics of environmental friendliness and effective beneficiation, has received more attention. Previous reports indicated that suspension magnetization roasting technology is an effective application in recovering refractory low-grade iron ore [36–39].

A suspension magnetization roasting and magnetic separation process of limonite ore was systematically investigated in this study. The experiments of roasting temperature, roasting time, reducing gas concentration, and magnetic intensity were conducted. During the suspension magnetization roasting process, the phase transformation, magnetism variation, and microstructure evolution were studied using X-ray diffraction (XRD), vibrating sample magnetometer (VSM), and scanning electron microscope (SEM).

2. Materials and Methods

2.1. Materials

The limonite ore used in the study was obtained from Kunming, China. The sample had a particle size of 60 wt.% particles less than 74 μm. Chemical composition analysis and X-ray powder diffraction of the sample are shown in Table 1 and Figure 1, respectively.

As shown in Table 1, the iron content was 34.50%, and the FeO content was less than 0.10%. In addition, the contents of SiO_2, CaO, MgO, and Al_2O_3 were 34.12%, 0.27%, 0.37%, and 2.40%, respectively. Meanwhile, the content of harmful element P was 0.70%. The loss on ignition (LOI) was 6.99%.

As shown in Figure 1, the main iron minerals in the ore were goethite and hematite, and the main gangue minerals were quartz and polylithionite. A chemical phase analysis of iron was performed to determine the main phase composition of the sample. The analysis results are shown in Table 2.

Table 1. Analysis of the chemical composition of the limonite ore (mass, %).

Element	TFe	FeO	SiO_2	CaO	MgO	Al_2O_3	S	P	LOI
Content	34.50	<0.10	34.12	0.27	0.37	2.40	<0.004	0.70	6.99

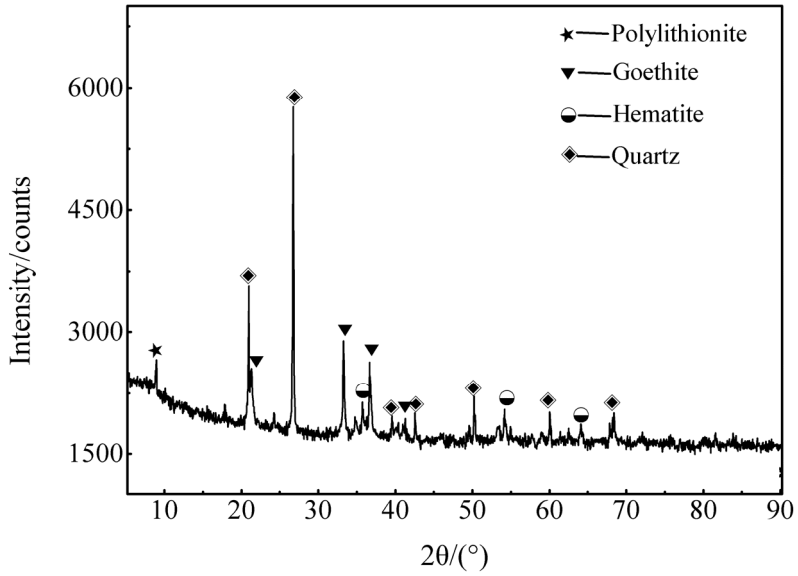

Figure 1. XRD pattern of the limonite ore.

Table 2. Chemical iron phase analysis of the limonite ore (mass, %).

Iron Phase	Iron in Magnetite	Iron in Hematite-Limonite	Iron in Siderite	Iron in Sulfide	Iron in Silicate	Total Iron
Mass	0.00	34.28	0.03	0.05	0.14	34.50
Distribution rate	0.00	99.36	0.09	0.14	0.41	100.00

As shown in Table 2, iron mainly existed in the form of limonite and hematite, and the distribution rate of iron was 99.36%, which was consistent with the analysis results in Figure 1. In addition, the distribution rates of iron in siderite, sulfide, and silicate were 0.09%, 0.14%, and 0.41%, respectively.

The morphological characteristics of each mineral particle in the ore have an important influence on the dissociation of the mineral. The intergrowth relationship and distribution characteristics between useful minerals and gangue minerals in raw ore were investigated by optical microscopy. The analysis is shown in Figure 2. Limonite was mainly distributed in the gangue in granular, massive, and disseminated forms as shown in Figure 2a–c. In addition, the cavities of the limonite were covered with gangue minerals. The hematite content in the ore was high, and the distribution was concentrated. Hematite was mostly produced in radial, fibrous, scaly, and granular shapes, and a small amount was produced in plate, flake, radial, filament, and needle-like shapes, as shown in Figure 2d,e. It was often a dense aggregate, a small amount of which was disseminated in the gangue (Figure 2f). These results indicated a complicated relationship between useful minerals (limonite and hematite) and gangue minerals. It is difficult to effectively separate limonite and hematite from gangue minerals.

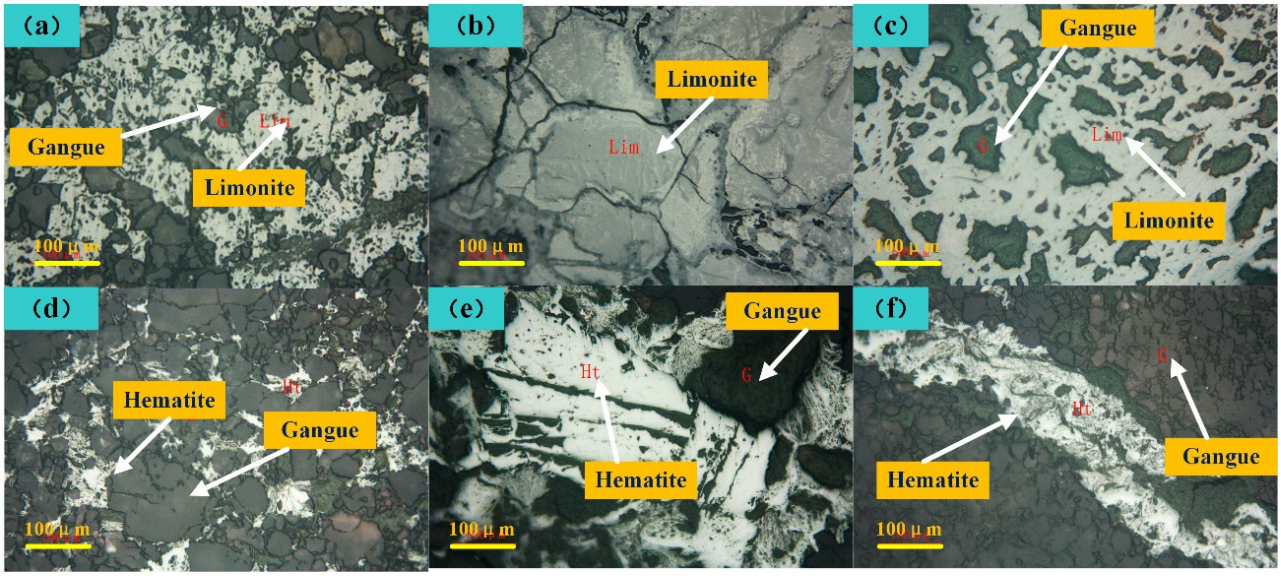

Figure 2. Distribution characteristics of the main minerals in the ore: (**a**–**c**) denote the limonite inlay structure; (**d**–**f**) denote the inlay structure of hematite.

2.2. Experimental Equipment and Methods

The limonite ore was first crushed to −2 mm using a double roller crusher and then ground to 60 wt.% passing 74 μm by a ball mill. A suspension magnetization roasting system consisting of a small vertical tube furnace (OTF-1200X-S-VT, HF-Kejing Hefei China), a multichannel proton flowmeter control system (GSL-LCD, HF-Kejing Hefei China), and gas supply equipment was used in this study. Three parallel experiments were carried out for the conditional experiments of the suspension magnetization roasting process. Each error bar represents the mean ± SD of triplicate samples.

First, high-purity nitrogen gas with a total gas flow of 600 mL/min was used to empty the air in the furnace tube. When the vertical tube furnace reached the required temperature, the prepared sample was put into the furnace tube. Second, the mixture of reducing gas (CO gas and H_2 gas) was passed into the furnace tube according to the designed concentration, and a total gas flow of 600 mL/min was kept constant during the magnetic roasting process (the calculation for the mixture of reducing gas concentration is shown in Equation (1)). When the specified roasting time was reached, the reducing gas was stopped, and the furnace tube was removed for cooling to room temperature using nitrogen as a protective gas at the same time. The cooled roasted products were ground to the required particle size; subsequently, low-intensity magnetic separation experiments were carried out using a magnetic separation tube (XCSG–120). After magnetic separation, the magnetic product was the final concentrate, and the nonmagnetic product was the tailings. The iron grade of the concentrate and tailings were detected by the laboratory using chemical analysis methods, and the recovery of iron was calculated according to Equation (2). According to the characteristics of suspension magnetization roasting, the influences of roasting temperature, roasting time, and reducing gas concentration on the magnetization roasting process were investigated.

$$C_R = (Q_{CO} + Q_H)/(Q_N + Q_{CO} + Q_H) \times 100\% \quad (1)$$

where C_R is the reducing gas concentration and Q_{CO}, Q_H, and Q_N are the CO, H_2, and N_2 flow rates, respectively.

$$\varphi = (\beta/\alpha)\cdot(\alpha - \theta)/(\beta - \alpha) \times 100\% \quad (2)$$

where α, β, and θ are the iron grades of the raw sample, magnetic concentrates, and tailings, respectively, and φ is the iron recovery.

2.3. Sample Analysis Methods

In this study, the mineralogical composition of raw samples, roasted products, and magnetic separation products was detected by a polycrystalline X-ray diffractometer (PW3040, PANalytical B.V., Almelo, The Netherlands). The polycrystalline X-ray diffractometer was equipped with a 2.2 kW Cu anode with a long, fine-focus ceramic X-ray tube for generating Cu Ka radiation. Its operating parameters were as follows: tube voltage 40 kV, tube current 40 mA, scanning range, 2θ range = 5–90°, step scanning, step length 0.033°, dwell time 20.68 s, wavelength 0.1541 nm, scanning speed 12°·min^{-1}, and operating temperature 298 K. Then, the XRD patterns were analyzed using the software package HighScore Plus. Powder diffraction file (PDF) database and the standard data card JCPDS cards were used for qualitative phase analysis of sample data during the analysis process. Finally, the analyzed data without noise reduction was plotted using OriginPro 8.5 software. The iron phase of samples was analyzed by physical and chemical methods [3].

A field emission scanning electron microscope (Zeiss Ultra Plus, Zeiss Microscopy Co., Ltd., Jena, Germany) equipped with Energy Dispersive Spectrometer (EDS) analyses was used to analyze the micromorphology of the reduced samples. The working parameters were as follows: acceleration voltage 15 Kv; magnification was set according to actual demand. The SE2 and BSE modes were used to collect images, the EDS energy spectrum was used to collect the elements on the surface of the sample, and the instrument's SmartSEM software (Version 5.05) was used to analyze the collected images and energy spectrum data. In the data analysis process, the EDS energy spectrum data was quantitatively analyzed according to the relative mass content and relative atomic number content of the elements.

A vibrating sample magnetometer (JDAW2000D, Changchun, China) was used to detect the magnetic properties of raw samples, roasted products, and magnetic separation products. The initial magnetization curves and hysteresis loops of the samples were tested in magnetizing magnetic field intensity ranges of 0 kA·m^{-1} to 800 kA·m^{-1} and −800 kA·m^{-1} to 800 kA·m^{-1}, respectively. The specific magnetization coefficient curves of the samples were obtained by analyzing the initial magnetization curves according to Equation (8).

$$\chi = M_b / H_b \tag{3}$$

where M_b and H_b are the specific magnetization and the external magnetic field strength, respectively, and χ is the specific magnetic susceptibility. The process flow diagram is shown in Figure 3.

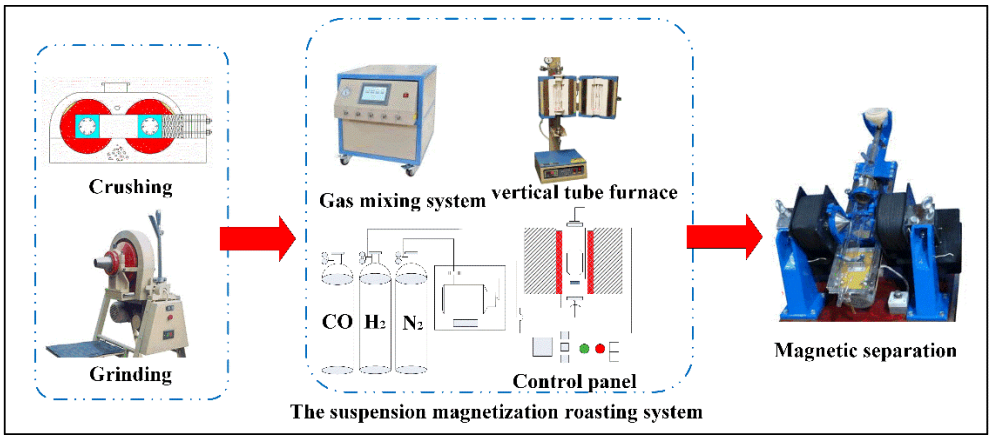

Figure 3. Flow chart of the experiment process.

3. Results and Discussion

3.1. Magnetization Roasting Experiments

3.1.1. Effect of Roasting Temperature

Temperature is a crucial influencing factor in the suspension magnetization roasting process. The effect of temperature on suspension magnetization roasting was investigated under the following conditions: a reducing gas concentration of 20% (CO concentration of 5%, H_2 concentration 15%), a reduction time of 12.5 min, a grinding size of 75 wt.% particles less than 43 μm, and a magnetic intensity of 85.17 kA/m. The effect of roasting temperature on the magnetic separation is shown in Figure 4a.

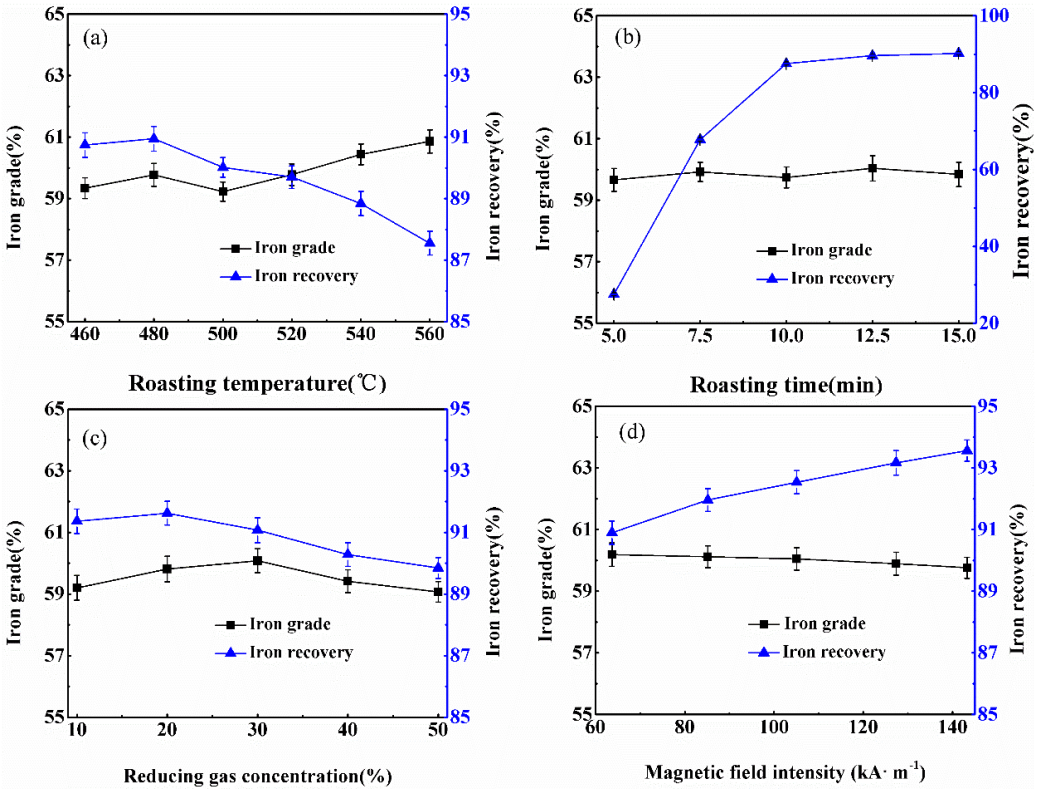

Figure 4. Effect of roasting conditions on the recovery and Fe grade of the magnetic concentrate: (**a**) roasting temperature, (**b**) roasting time, (**c**) reducing gas concentration, (**d**) magnetic field intensity.

As shown in Figure 4a, the iron grade of iron concentrate fluctuated slightly when the temperature increased from 460 °C to 500 °C. When the temperature increased from 500 °C to 560 °C, the iron grade of the concentrate gradually increased from 59.23% to 60.86%. Conversely, the iron recovery gradually decreased with increasing temperature; when the temperature increased from 480 °C to 560 °C, the iron recovery decreased from 90.95% to 87.55%. The test results showed that an increase in temperature could improve the magnetization roasting process. However, an excessively high temperature will cause an over-reduction as in Equations (4) and (5), and the formation of wustite (FeO) will further affect the magnetic separation of roasted products, resulting in a decrease in iron recovery. Therefore, the appropriate roasting temperature was determined to be 480 °C, and an iron concentrate with iron grade of 59.77% and recovery of 90.95% was obtained.

$$Fe_3O_4 + H_2(g) = 3FeO + H_2O(g) \quad (4)$$

$$Fe_3O_4 + CO(g) = 3FeO + CO_2(g) \quad (5)$$

3.1.2. Effect of Roasting Time

The effect of roasting time on suspension magnetization roasting was investigated under the following conditions: a reducing gas concentration of 20% (CO concentration of 5%, H_2 concentration 15%), a reduction temperature of 480 °C, a grinding size of 75 wt.% particles less than 43 μm, and a magnetic intensity of 85.17 kA/m. The effect of roasting time on the iron concentrate grade and iron recovery is presented in Figure 4b.

As shown in Figure 4b, the iron recovery of magnetic concentrate increased rapidly with an increase in roasting time. When the roasting time was extended from 5 min to 10 min, the recovery of iron concentrate increased rapidly from 27.53% to 89.61%. As the roasting time continued to increase, the iron recovery of concentrate gradually slowed down. Meanwhile, the iron grade of magnetic concentrate fluctuated slightly when the roasting time increased from 5 min to 15 min. Therefore, the appropriate roasting time is determined to be 12.5 min, and an iron concentrate with iron grade of 60.04% and recovery of 89.06% was obtained.

3.1.3. Effect of Reducing Gas Concentration

The effect of reducing gas concentration on magnetization roasting was investigated by a reducing gas concentration from 10% to 50%, a roasting temperature of 480 °C, and a reduction time of 12.5 min, a grinding size of 75 wt.% particles less than 43 μm, and a magnetic intensity of 85.17 kA/m. The effect of reducing gas concentration on the iron grade and recovery of iron concentrate is shown in Figure 4c.

As shown in Figure 4c, as the concentration of reducing gas increased, iron grade and recovery first increased and then decreased. The iron recovery reached the maximum of 91.62% when the reducing gas concentration was 20%. As the reducing gas concentration continued to increase, the iron recovery began to decrease. This is because excess reducing gas leads to the formation of FeO, which lowers the iron recovery of subsequent magnetic separation. Therefore, the appropriate reducing gas concentration was determined to be 20%.

3.1.4. Effect of Magnetic Field Intensity

The effect of magnetic field intensity was investigated under the following conditions: a roasting temperature of 480 °C, a reducing gas concentration of 20% (CO concentration of 5%, H_2 concentration 15%), a reduction time of 12.5 min, and a grinding size of 75 wt.% particles less than 43 μm. The results are shown in Figure 4d.

As shown in Figure 4d, the iron recovery increased from 90.90% to 93.56% when the magnetic field intensity increased from 63.7 kA/m to 143.3 kA/m. Conversely, a decrease in iron grade occurred as the magnetic field intensity increased. This trend may be due to the magnetic agglomeration during magnetic separation process, in which some gangue minerals are mixed in the magnetic concentrate, resulting in a decrease in iron grade. Therefore, the suitable magnetic field intensity was determined to be 85.17 kA/m, and the iron grade and recovery of the concentrate were 60.12% and 91.96%, respectively.

3.2. Phase Transformation

The phase transformation process of the sample during the magnetization roasting process was studied in detail through XRD. The XRD patterns of raw ore, roasted products, and iron concentrate were compared and analyzed. The results are plotted in Figure 5.

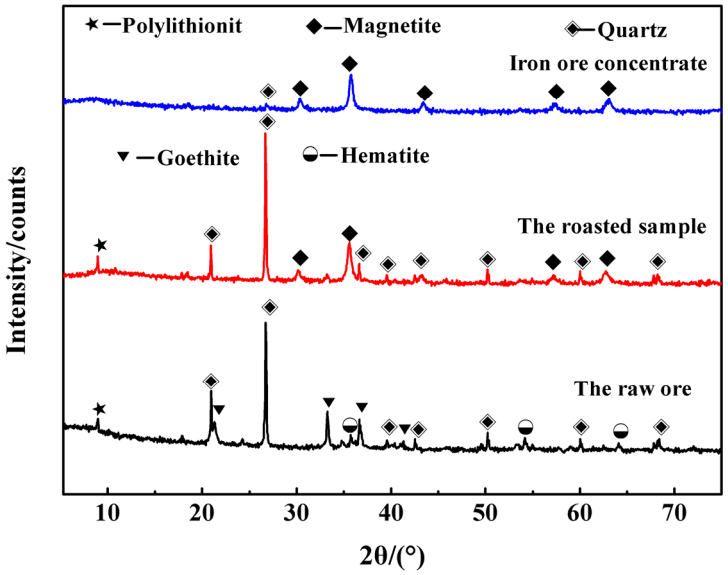

Figure 5. XRD pattern analysis of raw ore, roasted sample, and iron ore concentrate.

As shown in Figure 5, the iron in the raw ore mainly existed in the form of goethite and hematite. Compared with the raw ore samples, the diffraction peak of iron minerals in roasted samples was only magnetite, which indicated that the goethite and hematite in the sample were converted to magnetite in the magnetization roasting process; simultaneously, the magnetite in the roasted product could be recovered by low-intensity magnetic separation. In addition, there was still a small amount of quartz in iron concentrate, and this part of quartz can be further removed by the flotation process.

$$Fe_2O_3 \cdot nH_2O = Fe_2O_3 + nH_2O(g) \quad (6)$$

$$3Fe_2O_3 + CO(g) = 2Fe_3O_4 + CO_2(g) \quad (7)$$

$$3Fe_2O_3 + H_2(g) = 2Fe_3O_4 + H_2O(g) \quad (8)$$

The phase transformation under different roasting times is shown in Figure 6. Compared with the XRD pattern of the raw ore, when the roasting time was 5 min, the diffraction peak of goethite disappeared, and goethite was transformed into hematite by dehydration as in Equation (6). With the increase in roasting time, the diffraction peaks intensity of hematite gradually weakened, some diffraction peaks of hematite gradually vanished, and the diffraction peaks of magnetite gradually appeared. When the roasting time was 12.5 min, the diffraction peak of hematite disappeared completely, and the primary iron mineral was magnetite. This indicated that the goethite and hematite in the raw ore could be converted into magnetite in magnetization roasting.

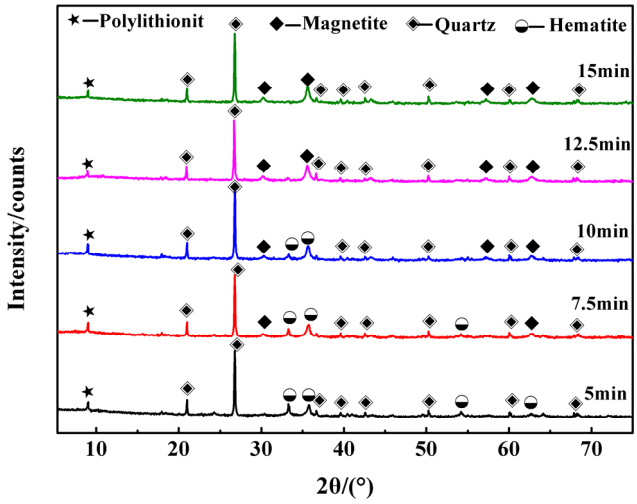

Figure 6. XRD analysis of roasted samples at different roasting times.

3.3. Magnetism Analysis

The magnetism properties of roasted products at different roasting times were studied using VSM, and the results were shown in Figures 7–9. As the roasting time extended from 5 min to 15 min, the saturation magnetization increased from 16.42 Am^2/kg to 30.71 Am^2/kg, and the magnetic susceptibility maximum increased from 1.67 $\times$ 10^{-4} m^3/kg to 2.88 $\times$ 10^{-4} m^3/kg in this process. Moreover, when the roasting time was 12.5 min, the roasted product with saturation magnetization of 30.10 Am^2/kg and maximum magnetic susceptibility of 2.85 $\times$ 10^{-4} m^3/kg was obtained. The magnetism variation in magnetization roasting was mainly due to the formation of magnetite, which is a ferrimagnetic mineral. Thus, the magnetism of roasted products significantly improved in this process with the increase in the content of magnetite.

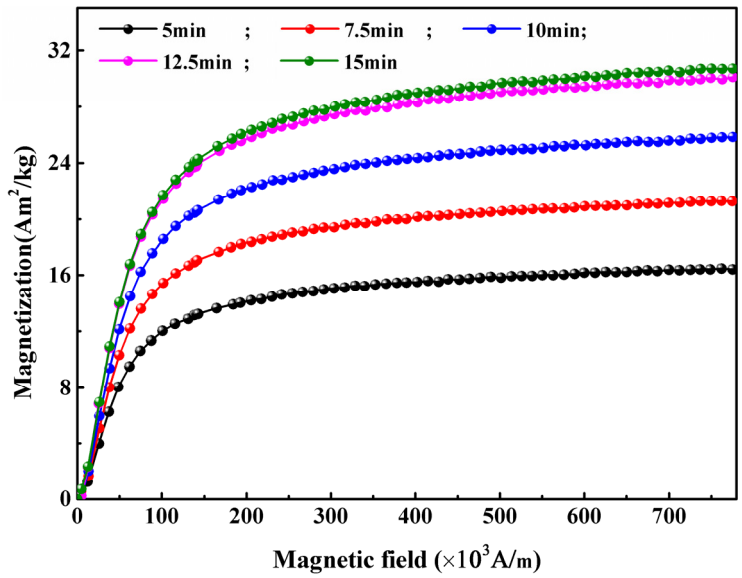

Figure 7. Magnetization curves of roasted products.

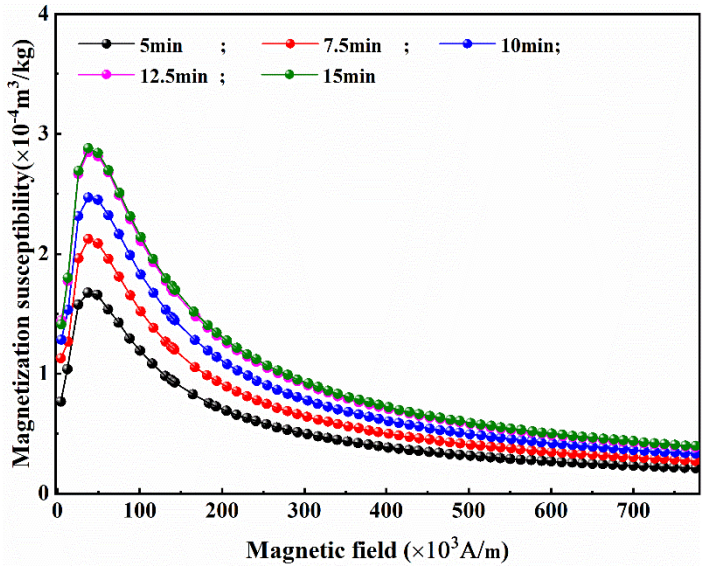

Figure 8. Magnetic susceptibility curves of roasted products.

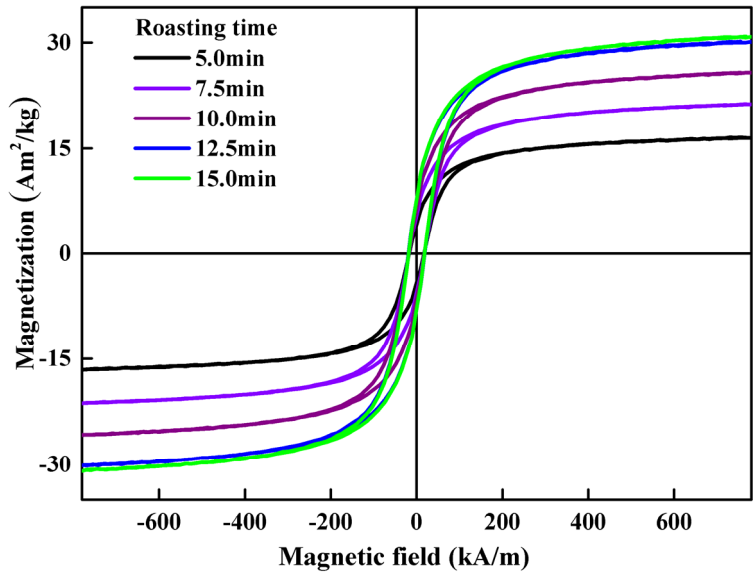

Figure 9. Hysteresis loops of roasted products.

3.4. Microstructure Evolution Analysis

The microscopic morphology changes of the raw ore and roasted ore were observed using SEM-EDS, and the results were shown in Figure 10. As Figure 10a,b show, the appearance of iron mineral particles was a flaky structure, and the surface was relatively flat, without cracks. The iron minerals had radial and needle-like shapes in the internal cross-section; simultaneously, the inside of the section was relatively dense, with almost no cracks or pores. As shown in Figure 10e,f, with a roasting time of 3 min, cracks began to appear on the surface of mineral particles, while cracks and pores appeared inside the particles. The appearance of this phenomenon was related to the dehydration and decomposition of goethite in high-temperature roasting. As shown in Figure 10g,h, with the extension of the roasting time, tiny cracks on the surface of the mineral particles continued to develop and formed large cracks. Simultaneously, cracks appeared inside the ore particles, and the number of internal pores also increased. This phenomenon could be mainly due to the rapid release of water vapor and CO_2 generated by the rapid reactions of reducing gases with hematite.

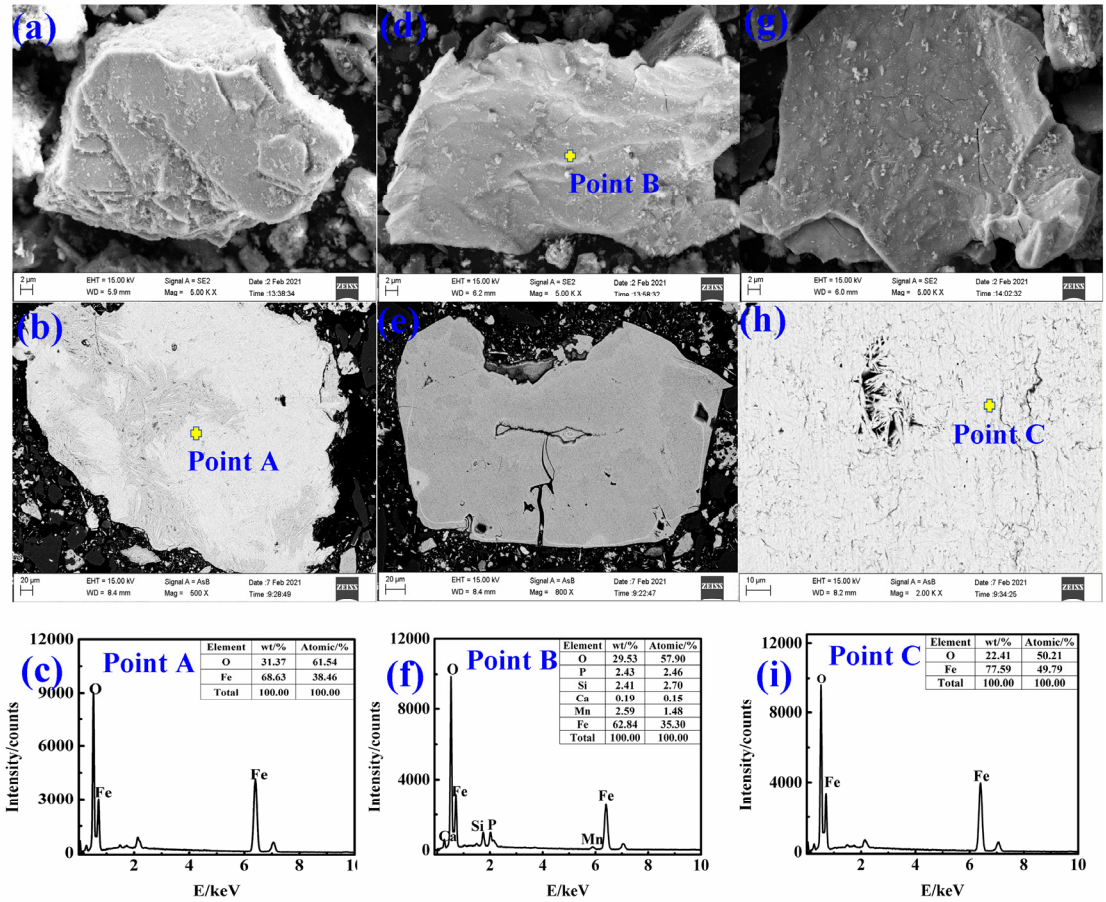

Figure 10. SEM–EDS analysis of raw ore and roasted products: (**a**–**c**) raw ore; (**d**–**f**) roasted product of 3 min; (**g**–**i**) roasted product of 12.5 min.

4. Conclusions

(1) This research demonstrated that limonite and hematite were reduced to magnetite in the suspension magnetization roasting process. The optimal conditions were determined as a reduction temperature of 480 °C, reducing gas of CO and H_2 with a concentration of 20%, reducing time of 12.5 min, magnetic intensity of 85.17 kA/m, and an iron concentrate with iron grade of 60.12% and recovery of 91.96% was obtained.

(2) XRD and SEM–EDS analysis results indicated that goethite dehydrated to hematite in high-temperature roasting; then hematite was transformed into magnetite with the reducing gas. Pores and cracks appeared on the surface and inside of the ore particle, which is conducive to the reduction reaction. Based on the VSM analysis, the magnetism of roasted products significantly improved in magnetization roasting, which is due to the formation of ferrimagnetic magnetite.

Author Contributions: Conceptualization, J.J. and X.Z.; data curation, P.L.; formal analysis, P.L.; funding acquisition, Y.H. and X.Z.; investigation, P.L.; project administration, Y.H. and Y.L.; writing—original draft, P.L.; writing—review & editing, J.J. All authors have read and agreed to the published version of the manuscript.

Funding: National Natural Science Foundation of China (Nos. 52104249, 51734005, 51874071), and China Postdoctoral Science Foundation (No. 2021M700726).

Acknowledgments: This work was financially supported by National Natural Science Foundation of China (Nos. 52104249, 51734005, 51874071), and China Postdoctoral Science Foundation (No. 2021M700726), for which the authors express their appreciation.

Conflicts of Interest: The authors declare no conflict of interest.

References

1. Laguna, C.; González, F.; García-Balboa, C.; Ballester, A.; Blázquez, M.; Muñoz, J.A. Bioreduction of iron compounds as a possible clean environmental alternative for metal recovery. *Miner. Eng.* **2011**, *24*, 10–18. [CrossRef]
2. Nakhaei, F.; Irannajad, M. Reagents types in flotation of iron oxide minerals: A review. *Miner. Process. Extr. Met. Rev.* **2017**, *39*, 89–124. [CrossRef]
3. Zhang, X.; Han, Y.; Sun, Y.; Li, Y. Innovative utilization of refractory iron ore via suspension magnetization roasting: A pilot-scale study. *Powder Technol.* **2019**, *352*, 16–24. [CrossRef]
4. Yu, J.-W.; Han, Y.-X.; Li, Y.-J.; Gao, P. Growth behavior of the magnetite phase in the reduction of hematite via a fluidized bed. *Int. J. Miner. Met. Mater.* **2019**, *26*, 1231–1238. [CrossRef]
5. Wang, Y.-Z.; Zhang, J.-L.; Liu, Z.-J.; Du, C.-B. Recent Advances and Research Status in Energy Conservation of Iron Ore Sintering in China. *JOM* **2017**, *69*, 2404–2411. [CrossRef]
6. USGS. *Mineral Commodity Summaries 2021*; U.S. Geological Survey: Reston, VA, USA, 2021; pp. 88–90.
7. Yuan, S.; Zhou, W.; Han, Y.; Li, Y. Selective enrichment of iron particles from complex refractory hematite-goethite ore by coal-based reduction and magnetic separation. *Powder Technol.* **2020**, *367*, 305–316. [CrossRef]
8. Peng, T.; Gao, X.; Li, Q.; Xu, L.; Luo, L.; Xu, L. Phase transformation during roasting process and magnetic beneficiation of oolitic-iron ores. *Vacuum* **2017**, *146*, 63–73. [CrossRef]
9. Tang, Z.; Gao, P.; Li, Y.; Han, Y.; Li, W.; Butt, S.; Zhang, Y. Recovery of iron from hazardous tailings using fluidized roasting coupling technology. *Powder Technol.* **2020**, *361*, 591–599. [CrossRef]
10. Zhang, Q.; Sun, Y.; Han, Y.; Li, Y. Pyrolysis behavior of a green and clean reductant for suspension magnetization roasting. *J. Clean. Prod.* **2020**, *268*, 122173. [CrossRef]
11. Zhang, K.; Ge, Y.; Guo, W.; Li, N.; Wang, Z.; Luo, H.; Hu, Q.; Li, B.; Wu, W.; Shang, S. Phase transition and magnetic properties of low-grade limonite during reductive roasting. *Vacuum* **2019**, *167*, 163–174. [CrossRef]
12. Mochizuki, Y.; Tsubouchi, N. Upgrading Low-Grade Iron Ore through Gangue Removal by a Combined Alkali Roasting and Hydrothermal Treatment. *ACS Omega* **2019**, *4*, 19723–19734. [CrossRef] [PubMed]
13. Wu, F.; Cao, Z.; Wang, S.; Zhong, H. Novel and green metallurgical technique of comprehensive utilization of refractory limonite ores. *J. Clean. Prod.* **2018**, *171*, 831–843. [CrossRef]
14. Pownceby, M.I.; Hapugoda, S.; Manuel, J.; Webster, N.A.; MacRae, C. Characterisation of phosphorus and other impurities in goethite-rich iron ores—Possible P incorporation mechanisms. *Miner. Eng.* **2019**, *143*, 106022. [CrossRef]
15. Zhu, D.-Q.; Wang, H.; Pan, J.; Yang, C.-C. Influence of Mechanical Activation on Acid Leaching Dephosphorization of High-phosphorus Iron Ore Concentrates. *J. Iron Steel Res. Int.* **2016**, *23*, 661–668. [CrossRef]
16. Agrawal, S.; Dhawan, N. Microwave Carbothermic Reduction of Low-Grade Iron Ore. *Met. Mater. Trans. A* **2020**, *51*, 1576–1586. [CrossRef]
17. Donskoi, E.; Collings, A.; Poliakov, A.; Bruckard, W. Utilisation of ultrasonic treatment for upgrading of hematitic/goethitic iron ore fines. *Int. J. Miner. Process.* **2012**, *114–117*, 80–92. [CrossRef]
18. Filippov, L.; Silva, K.; Piçarra, A.; Lima, N.; Santos, I.; Bicalho, L.; Filippova, I.; Peres, A. Iron Ore Slimes Flotation Tests Using Column and Amidoamine Collector without Depressant. *Minerals* **2021**, *11*, 699. [CrossRef]
19. Silva, K.; Filippov, L.O.; Piçarra, A.; Flilippova, I.V.; Lima, N.; Skliar, A.; Faustino, L.; Filho, L.L. New perspectives in iron ore flotation: Use of collector reagents without depressants in reverse cationic flotation of quartz. *Miner. Eng.* **2021**, *170*, 107004. [CrossRef]
20. Matiolo, E.; Couto, H.J.B.; Lima, N.; Silva, K.; de Freitas, A.S. Improving recovery of iron using column flotation of iron ore slimes. *Miner. Eng.* **2020**, *158*, 106608. [CrossRef]
21. Lima, N.P.; Silva, K.; Souza, T.; Filippov, L. The Characteristics of Iron Ore Slimes and Their Influence on The Flotation Process. *Minerals* **2020**, *10*, 675. [CrossRef]
22. Panda, L.; Biswal, S.K.; Venugopal, R.; Mandre, N.R. Recovery of Ultra-Fine Iron Ore from Iron Ore Tailings. *Trans. Indian Inst. Met.* **2017**, *71*, 463–468. [CrossRef]
23. Yin, W.; Tang, Y. Interactive effect of minerals on complex ore flotation: A brief review. *Int. J. Miner. Metall. Mater.* **2020**, *27*, 571–583. [CrossRef]
24. Dubey, A.; Patra, A.S.; Sarkar, A.N.; Basu, A.; Tripathy, S.K.; Mukherjee, A.; Bhatnagar, A. Synthesis of a copolymeric system and its flocculation performance for iron ore tailings. *Miner. Eng.* **2021**, *165*, 106848. [CrossRef]
25. Li, M.; Xiang, Y.; Chen, T.; Gao, X.; Liu, Q. Separation of ultra-fine hematite and quartz particles using asynchronous flocculation flotation. *Miner. Eng.* **2021**, *164*, 106817. [CrossRef]
26. Roy, S.; Nayak, D.; Rath, S.S. A review on the enrichment of iron values of low-grade Iron ore resources using reduction roasting-magnetic separation. *Powder Technol.* **2020**, *367*, 796–808. [CrossRef]
27. Yu, J.; Han, Y.; Li, Y.; Gao, P. Recent Advances in Magnetization Roasting of Refractory Iron Ores: A Technological Review in the Past Decade. *Miner. Process. Extr. Met. Rev.* **2019**, *41*, 349–359. [CrossRef]
28. Nanda, D.; Mandre, N.R. Studies on Characterization and Beneficiation of Typical Low-Grade Goethitic Iron Ore Jharkhand, India. *Trans. Indian Inst. Met.* **2018**, *71*, 2985–2992. [CrossRef]
29. Fu, Y.-F.; Yin, W.-Z.; Yang, B.; Li, C.; Zhu, Z.-L.; Li, D. Effect of sodium alginate on reverse flotation of hematite and its mechanism. *Int. J. Miner. Met. Mater.* **2018**, *25*, 1113–1122. [CrossRef]

30. Man, Y.; Feng, J.-X. Effect of iron ore-coal pellets during reduction with hydrogen and carbon monoxide. *Powder Technol.* **2016**, *301*, 1213–1217. [CrossRef]
31. Gao, P.; Li, G.-F.; Han, Y.-X.; Sun, Y.-S. Reaction Behavior of Phosphorus in Coal-Based Reduction of an Oolitic Hematite Ore and Pre-Dephosphorization of Reduced Iron. *Metals* **2016**, *6*, 82. [CrossRef]
32. Li, G.; Liu, M.; Rao, M.; Jiang, T.; Zhuang, J.; Zhang, Y. Stepwise extraction of valuable components from red mud based on reductive roasting with sodium salts. *J. Hazard. Mater.* **2014**, *280*, 774–780. [CrossRef] [PubMed]
33. Faris, N.; Tardio, J.; Ram, R.; Bhargava, S.; Pownceby, M.I. Investigation into coal-based magnetizing roasting of an iron-rich rare earth ore and the associated mineralogical transformations. *Miner. Eng.* **2017**, *114*, 37–49. [CrossRef]
34. Sahu, S.N.; Baskey, P.K.; Barma, S.D.; Sahoo, S.; Meikap, B.; Biswal, S.K. Pelletization of synthesized magnetite concentrate obtained by magnetization roasting of Indian low-grade BHQ iron ore. *Powder Technol.* **2020**, *374*, 190–200. [CrossRef]
35. Rath, S.S.; Rao, D.S.; Tripathy, A.; Biswal, S.K. Biomass briquette as an alternative reductant for low grade iron ore resources. *Biomass Bioenergy* **2018**, *108*, 447–454. [CrossRef]
36. Yuan, S.; Liu, X.; Gao, P.; Han, Y. A semi-industrial experiment of suspension magnetization roasting technology for separation of iron minerals from red mud. *J. Hazard. Mater.* **2020**, *394*, 122579. [CrossRef]
37. Li, Y.; Zhang, Q.; Yuan, S.; Yin, H. High-efficiency extraction of iron from early iron tailings via the suspension roasting-magnetic separation. *Powder Technol.* **2021**, *379*, 466–477. [CrossRef]
38. Liu, X.; Gao, P.; Yuan, S.; Lv, Y.; Han, Y. Clean utilization of high-iron red mud by suspension magnetization roasting. *Miner. Eng.* **2020**, *157*, 106553. [CrossRef]
39. Yuan, S.; Zhou, W.; Han, Y.; Li, Y. Efficient enrichment of iron concentrate from iron tailings via suspension magnetization roasting and magnetic separation. *J. Mater. Cycles Waste Manag.* **2020**, *22*, 1152–1162. [CrossRef]